

Enhanced self-collimation effect by low rotational symmetry in hexagonal lattice photonic crystals.

Mehmet Z. Yüksel¹, Hasan Oguz¹, Önder O. Karakılınc², Halil Berberoğlu³, Mirbek Turduev⁴,
Muzaffer Adak¹, Sevgi K. Ozdemir¹

¹Department of Physics, Pamukkale University, Denizli, Türkiye.

²Department of Electrical-Electronics Engineering, Pamukkale University, Denizli, Türkiye.

³ Department of Physics, Ankara Hacı Bayram Veli University, Ankara, Türkiye.

⁴Department of Electrical and Electronics Engineering, Kyrgyz-Turkish Manas University,
Bishkek, Kyrgyzstan.

ABSTRACT: In this study, we present the design of a photonic crystal (PC) structure with a hexagonal lattice, where adjustments to the PC unit cell symmetry reveal an all-angle self-collimation (SC) effect. By optimizing opto-geometric parameters, such as the rotational angle of auxiliary rods and adjacent distances, we analyze the SC property in detail, leveraging group velocity dispersion (GVD) and third-order dispersion (TOD) characteristics. We also investigate the relationship between symmetry properties and their influence on dispersion characteristics. Through symmetry manipulation, we gain a comprehensive understanding of the underlying mechanisms governing light collimation and confinement in the proposed configurations. The PC structure with a C_1 symmetry group exhibits all-angle SC effect within the range of $a/\lambda=0.652$ and $a/\lambda=0.668$ normalized frequencies, with a bandwidth of $\Delta\omega/\omega_c = 2.4\%$. Further breaking the symmetry, transforming from C_1 to C_2 group symmetry, enhances the SC bandwidth to $\Delta\omega/\omega_c = 6.5\%$ and reveals the perfect linear equi-frequency contours (EFC) at two different frequency bands: all angle SC between $a/\lambda=0.616$ and $a/\lambda=0.656$ normalized frequencies in the 4th transverse magnetic (TM) band and between $a/\lambda=0.712$ and $a/\lambda=0.760$ in the 5th TM band. Here, GVD and TOD values vary between $7.3 (a/2\pi c^2) - 254.3 (a/2\pi c^2)$ and $449.2 (a^2/4\pi^2 c^3) - 1.3 \times 10^5 (a^2/4\pi^2 c^3)$ for the TM 4th band, respectively. Also, GVD and TOD values vary between $182.5 (a/2\pi c^2) - 71.3 (a/2\pi c^2)$ and $-24380(a^2/4\pi^2 c^3) - 9619 (a^2/4\pi^2 c^3)$ for the TM 5th band values. Additionally, we propose a composite/hybrid PC structure resembling C_2 group symmetry, where two auxiliary rods are replaced by rectangular photonic wires with the same refractive index and width equal to the diameter of auxiliary rods. This hybrid structure exhibits an all-angle SC effect with an operating bandwidth of $\Delta\omega/\omega_c = 11.7\%$, displays near-zero GVD and TOD performance and offers enhanced robustness against potential fabrication precision issues.

Keywords: Photonic crystal, self-collimation, symmetry reduction, low symmetry

1. Introduction

Photonic Crystals (PCs) are periodic optical structures that manipulates the light wave propagation according to the formed energy bands of the photons. The PC concept entered the literature in 1987 with the independent studies of E. Yablonovitch [1] and S. John [2]. Their pioneering study on

photonic bandgaps (PBGs) have received great attention because the propagation of electromagnetic waves at certain frequencies can be either prohibited or allowed, regardless of the polarization and propagation direction of electromagnetic waves. These properties lead to many interesting optical phenomena and applications by the photonic structures such as optical filters, PBG-based mirrors, demultiplexers, logic gates, etc., [3, 4]. In recent years, important properties such as negative refraction [5], super-prism [6], slow light, and self-collimation (SC) effects [7] have gathered great interest of researchers. Periodic modulation of the optical medium provokes the emergence of the SC phenomenon under appropriate opto-geometric circumstances. The diffraction-sensitive Gaussian beam in free space propagates through the periodic medium without broadening and retaining its spatial profile allowing light to be propagated by confining in PCs without the requirement of using any waveguides. This feature paves the way for an efficient transportation of light and offers important optical applications such as on-chip optical interconnects [8], beam steering [9], steering, bending [7], and light splitting [10]. Furthermore, this effect can be used to combine, route, and guiding light beams by minimizing optical power loss in communication systems [11]. Recently, an on-chip waveguide based on the SC phenomenon has been demonstrated in two-dimensional (2D) PCs [8], and several interesting applications, such as channel-less waveguiding, bending of light, beam splitter, analog-to-digital converter, optical switch, etc. have been introduced [12, 13]. SC features are beneficial in waveguides for beam orientation [14], beam splitters [15,16], polarization beam splitters [17], logic gates [18], switches [19, 20], and demultiplexers [21, 22].

In this study, we propose the design of PC structure with a hexagonal lattice by adjusting the unit cell symmetry to reveal all-angle SC effect. The main objective is to explore and manipulate various optical properties including group velocity dispersion (GVD), third-order dispersion (TOD), and self-collimation (SC). Also, the relationship between the symmetry properties of PCs and their influence on dispersion characteristics is investigated. By analyzing the potential for tuning the optical properties through symmetry manipulation, we ensured a comprehensive understanding of the underlying mechanisms that govern light collimation and confinement in the proposed configurations. It may pave the way for the development of advanced photonic devices that exhibit desired performances in terms of transmission efficiency, dispersion control, and self-collimation. Additionally, the effects of variation in lattice geometries and unit cell configurations on EFCs as well as photonic band structures are analyzed to achieve the desired optical behavior in the proposed structures.

2. Problem Definition and Methodology

The geometric diversity resulting from the symmetry reduction applied to PCs enriches their dispersion properties as well as spatial domain characteristics [23]. In general PCs with square/rectangular lattices are more widely explored and analyzed by using EFCs approach (dispersion engineering) compared to the hexagonal structures with low symmetry unit cells [7]. Here, higher refractive index contrast, lower group velocity dispersion, and larger photonic gaps of the hexagonal structure makes them more suitable for revealing the desired optical properties

such as self-collimating, super-prism, optical filtering and waveguiding [6, 12, 13] as compared with those of the square/rectangular lattice PCs. For this reason, the PC structure arranged in a hexagonal lattice is preferred to design low-symmetry PC configurations exhibiting inherent all-angle self-collimation characteristics, in this study. There are a few studies on the SC properties of hexagonal structures based on EFC engineering in literature. Photonic bandgaps, waveguides, SC properties, and negative refraction in hexagonal PC structures have been investigated [24, 25]. Unfortunately, manipulating rotational symmetry in hexagonal lattice PCs to enhance their dispersion behavior remains blurred. It is reported that interesting and applicable optical properties can be obtained by tuning the geometry of low symmetry introduced in the PC unit cell [21, 26, 27]. To the best of our knowledge, this work presents a detailed analysis of all-angle SC characteristics of the low symmetric PC structures ordered in hexagonal lattices by using the EFC engineering approach for the first time.

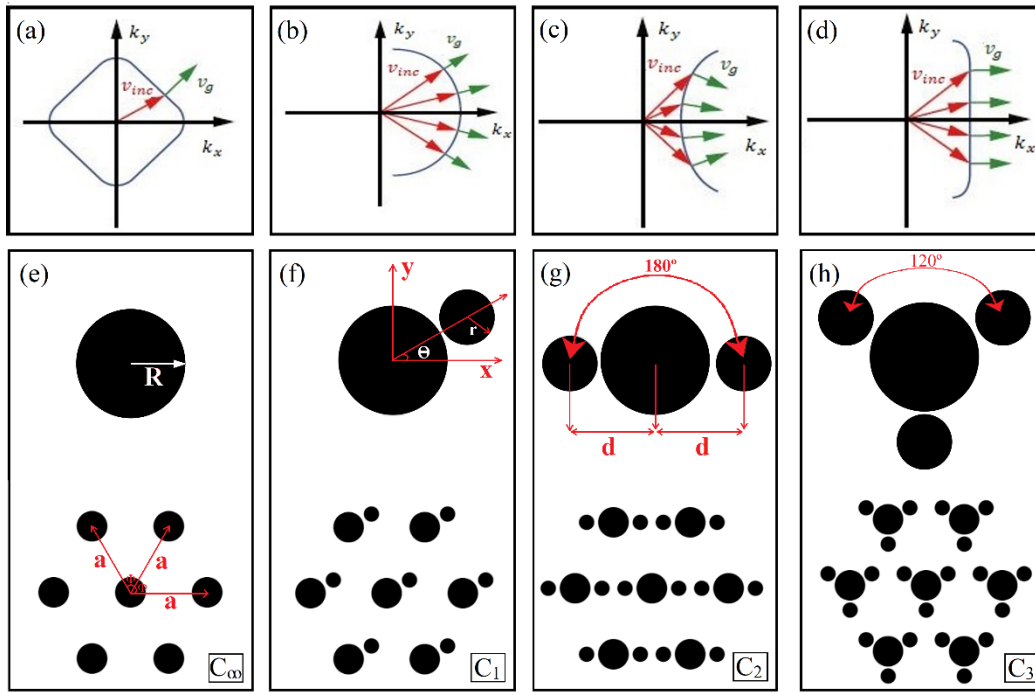


Figure 1. Wave propagation schemes under the analysis of EFC for (a) general arbitrary case, (b) homogeneous media, (c) medium exhibiting negative refraction effect, and (d) medium exhibiting self-collimation effect [30]. Schematic views of (e) hexagonal PC unit cell, (f) low rotational symmetric hexagonal PC unit cell with single auxiliary dielectric rod (C_1 symmetric structure) having rotational angle of θ , (g) two auxiliary dielectric rods (C_2 symmetric structure) and (h) three auxiliary dielectric rods (C_3 symmetric structure).

In this study, the plane wave expansion (PWE) method [28, 29] is applied to calculate the band structure of Bloch modes and EFCs analyses of the proposed low symmetry PC structures. Correspondingly, dispersion analyses are performed by using freely available MIT photonic bands (MPB) [30]. In the PWE method, Maxwell's equations are solved by taking account of an eigenvalue problem. Here, the angular frequencies of the modes in PCs stand for the eigenvalues, while the amplitude coefficients of the fields indicate the eigenvectors. Additionally, both

dielectric function and fields are introduced in the reciprocal k -space by using the Fourier series [31]. The projection of band structures on the k -space with constant frequencies can be expressed by EFCs. The curvature of EFCs in the k -space gives information/implications about the wave propagation behavior within/outside of the PC structure. Wave propagation schemes under analysis of EFC are represented in Fig. 1. As seen in Fig. 1(a), the incident wave with the velocity vector \vec{v}_{inc} (red arrow) leaves the PC interface perpendicularly to the group velocity \vec{v}_g (green arrow) due to the relation of $\vec{v}_g = \vec{\nabla}_k \omega(k)$ where $\omega(k)$ is the angular frequency at the wave vector k . Here, the group velocity of light represents the velocity of energy transport in the direction perpendicular to the EFCs within the PC structure. The schematic view of circular EFC is shown in Fig 1(b), where the light shows the wave propagation in an isotropic medium. In this case, the propagating wave does not undergo any diffraction. On the other hand, hyperbolic-shaped EFC produces negative refraction which results in a bi-refraction or focusing effect, as shown in Fig. 1(c). Also, the SC effect takes place when the wave passes through the flat EFC, as illustrated in Fig. 1(d) [32]. Here, the light of a specific wavelength propagates through a photonic structure with minimal diffraction, and angular dispersion. EFC presents linear shaped curves, as seen in Fig. 1(d) which indicates that the light propagates with a constant group velocity independent of incident light direction [33].

The finite-difference time-domain method (FDTD) is used to evaluate and extract spatial field distributions of the propagating wave within the PC structure [34, 35]. The PC structure ordered in hexagonal lattice is subjected to the periodic boundary conditions in two dimensions. Moreover, perfectly matched layers are applied to the simulation box to eliminate undesired boundary reflections [36]. As known, the dispersion characteristics of photonic structures with isolated unit cells (dielectric rods in air) are more susceptible to transverse-magnetic (TM) polarization modes, while fully connected ones (air holes in the dielectric slab) provide rich dispersion properties for transverse-electric (TE) polarization modes [30]. For this reason, throughout the study TM polarization mode is utilized to effectively manipulate and tailor EFCs.

In general, the periodicity of a geometrical configuration is defined as the repetition of basic structural components/units (unit cells) in a specific order. Additionally, the periodic structure is examined in terms of the types of symmetry present in space. In this context, PCs can be represented by utilizing the rotational symmetry of the unit cells, which are periodically distributed in space. Rotational symmetry determines the degree to which the unit cell must be rotated about its axis to reproduce the same structural view. The rotational symmetry group is symbolized by C_{rot} where the subscript “*rot*” represents the ratio of 2π radians to the amount of angle that needs to be rotated for the object [25]. The rotational symmetry groups analyzed in this study are depicted in Figs. 1(e) - 1(h). Here, Figs. 1(e) and 1(f) present fully symmetric structure and C_1 symmetry group, respectively.

3. Time and frequency domain analysis of self-collimation effect in hexagonal lattice with low symmetry PCs

The values of the dielectric constants for the PC rods shown in Fig. 1(e) and the air background medium are taken as $\epsilon_{PC} = 9.8$ and $\epsilon_{air} = 1.0$, respectively. The rods' radii are taken as $R = 0.2a$, where a is the lattice constant of the structure. The EFCs of 1st, 2nd, 3rd, and 4th bands for the TM polarization mode of the fully symmetric structure are created and presented in Figs. 2(a), 2(b), 2(c) and 2(d), respectively. As expected for the 1st band, there are perfect circular EFCs that exhibit the behavior of light propagation in a homogeneous medium. Also, much more complex situation appears for other bands. Especially SC effect is observed at the small incident angles for 2nd and 4th bands. However, there isn't any sign of the SC effect operating at wide incident angles. It reflects that one may obtain a special frequency response by tuning the lattice parameters (introducing a low symmetry effect into the PC unit cells) without breaking the structural lattice. As observed, the optical response of such structures is highly sensitive to the angular orientation of the components within the PC unit cell [23]. Through dispersion engineering, this sensitivity can be used to obtain desired optical properties [37, 38, 39]. For this reason, by introducing additional auxiliary dielectric rods having radii of $0.12a$ into fully symmetric hexagonal PC structure group C_{∞} is transformed into C_1 rotational symmetry group as represented in Fig. 1(f). The structural parameters of the PC structure with low symmetry are defined as the radii of the main dielectric rods (R), the radii of the auxiliary dielectric rods (r) and the distance between the centers of the main and auxiliary dielectric rods (d), as depicted in Figs. 1(e)-1(h). Dispersion characteristics of all the configurations considered in this study are examined by using PWE method. The inspections of the EFCs provide proper identification of the SC effect. Since all the opto-geometric parameters of PCs have strong effects on the appearance of linear shaped EFCs, the parametric optimizations are required to determine desired SC regions. In addition, to analyze the impact of low symmetry within the PC unit cell to tailoring of SC contours, there should be enough spatial place for freely adjustment of auxiliary rods. All of these pre-conditions force us to seek for the optimum opto-geometric parameters. By considering these restrictions, the radii of hexagonal lattice PCs are fixed to the optimized value of $R = 0.2a$ (this parameter is depicted in Fig. 1(e) as an inset). After taking the value of the $R = 0.2a$, the other parameters are scanned to obtain SC effect. The radii of auxiliary rods r and the distance d are scanned from $0.09a$ to $0.18a$ and $0.31a$ to $0.39a$, respectively. Finally, well defined radii and distance parameters are as follows $R = 0.2a$, $r = 0.12a$ and $d = 0.38a$, which display all-angle SC behavior of C_1 symmetry group. It is important to note that we analyze the all-angle SC effect only for the case of a rotational angle $\theta=0^\circ$ of auxiliary PC rods, ensuring conventional SC with light propagating in a non-angled direction.

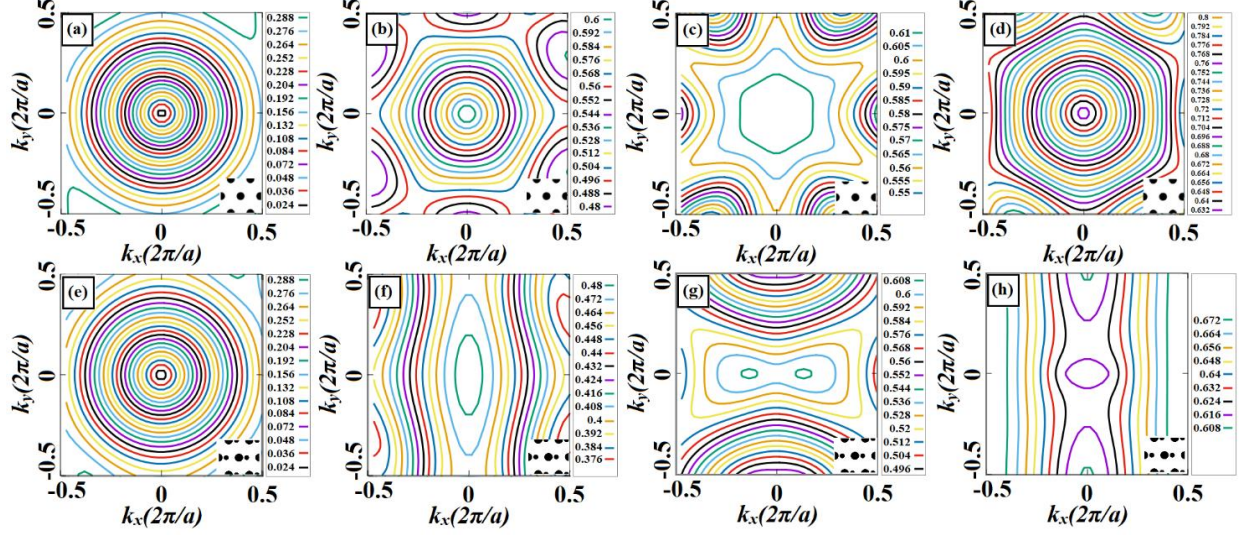


Figure 2. EFC plots of the hexagonal PC structure without dielectric rod (C_∞ symmetric structure) for (a) 1st, (b) 2nd, (c) 3rd and (d) 4th TM bands. EFCs for hexagonal PC structure with single auxiliary dielectric rod (C_1 symmetric structure) for (a) 1st, (b) 2nd, (c) 3rd and (d) 4th TM bands.

Figs. 2(e), 2(f), 2(g) and 2(h) show the EFC plots of 1st, 2nd, 3rd, and 4th bands, respectively. As expected, 1st band displays an isotropic medium effect as shown in Fig. 2 (a), but other bands take different shapes according to the introduced auxiliary rods which reshape EFCs different from those of fully symmetric structure. The 2nd band has semi-linear contours with wave diverging effect (see Fig. 2(f)) while the 3rd band shows a tight-angle SC effect in the propagation direction (EFCs having rectangular shape with curved corners) as shown in Fig. 2(g). On the other hand, the 4th band exhibits the desired SC effect for all incident angles at the normalized frequency region of $a/\lambda = 0.652$ and $a/\lambda = 0.668$. It is obvious that the analyzed structure can support the all-angle SC only at the narrowband with the bandwidth of $\Delta\omega/\omega = 2.4\%$. Also, presented EFCs are not completely linear at these frequencies. To investigate all-angle self-collimation effect in time domain, FDTD method is applied to the C_1 group symmetry PCs operating at the center frequency of $a/\lambda = 0.664$. Steady-state electric-field intensity distributions generated by the incident waves at the angles of 0° and 25° are presented in Figs. 3(a) and 3(b), respectively. As seen from these figures, the engineered SC effect operates for a wide range of angles. Here, regardless of the excitation angle of the incident wave, C_1 symmetry group PCs provide the propagation of light with negligible spatial broadening.

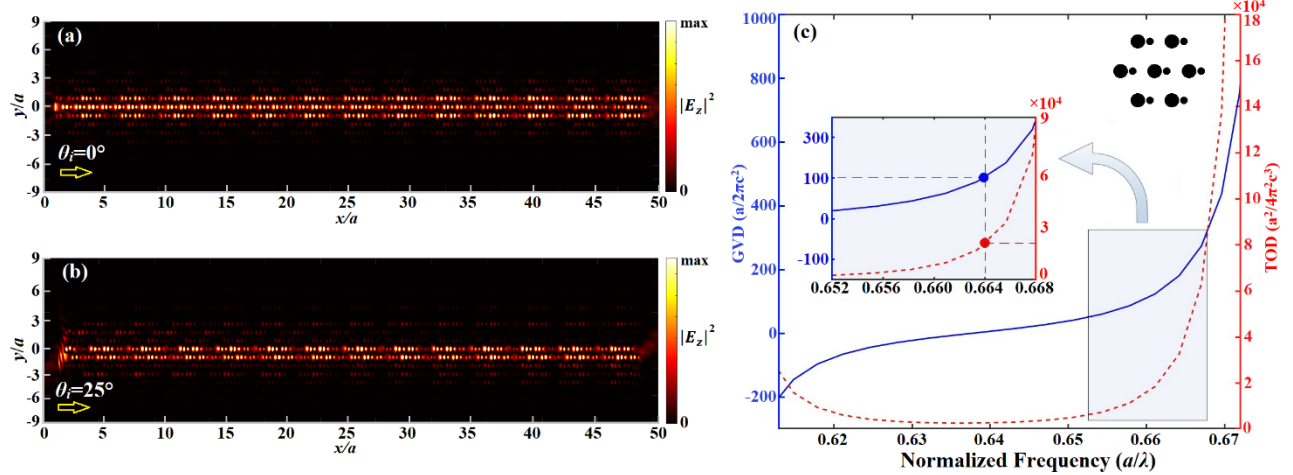


Figure 3. Steady-state electric field intensity distributions of C_1 symmetry group PC structure operating at a frequency of $a/\lambda=0.65$ under (a) 0° and (b) 25° incident light illumination. (c) Variation of the GVD and TOD values for the C_1 symmetry group PC structure as a function of normalized frequency, with representation of unit cell schematic as an inset.

It is also important to provide a qualitative analysis of the observed SC effect. Here, the quality of the SC effect is explored by utilizing GVD and TOD characteristics. GVD shows the dependence of group velocity on the optical wavelengths of light. GVD is defined as $\partial/\partial\omega(1/vg) = \partial^2 k/\partial\omega^2$, where k is the wave vector and ω is the angular frequency. It implies that the components of incident signal propagate at different velocities at each wavelength, which leads to temporal pulse broadening. The positive sign of GVD indicates to a normal distribution at which the group velocity decreases as the optical frequency increases, while the negative sign represents an anomalous distribution at which the group velocity rises with the optical frequency [40]. TOD is described by the derivative of GVD with respect to the angular frequency given as $\partial^3 k/\partial\omega^3$. It affects the shape of propagating pulse with a wide frequency spectrum. Regarding this matter, any PC structure that operates as a self-collimator should have as small as possible GVD and TOD values to avoid temporal dispersion and deformation of the propagated beam in a broad frequency range. Figure 3(c) illustrates the behavior of calculated GVD and TOD values for the proposed structure as a function of the normalized frequency. It is observed that GVD and TOD values are variate between $-200 (a/2\pi c^2)$ and $780 (a/2\pi c^2)$ and $10^4 (a^2/4\pi^2 c^3)$ and $18 \times 10^4 (a^2/4\pi^2 c^3)$ for the TM 4th band, respectively. As we are concentrated on the frequency range between $a/\lambda = 0.652$ and $a/\lambda = 0.668$ (see the inset in Fig. 3(c), which represents all-angle SC property), the values of GVD and TOD are obtained as $42.29 (a/2\pi c^2) - 390 (a/2\pi c^2)$ and $5.2 \times 10^3 (a^2/4\pi^2 c^3) - 9 \times 10^4 (a^2/4\pi^2 c^3)$, respectively. As seen, GVD gets relatively small value, which enables to generate the collimated beam. Although an incident beam is collimated during propagating the PC structure, the shape of the beam is distorted due to the relatively larger value of TOD. As a result, it can be reported that introducing low symmetry reveals all-angle SC effect in hexagonal PC structure. As known, the TOD takes small values when the variation of GVD with the frequency is smooth and nearly linear. Therefore, by adjusting the index contrast or

adding more auxiliary PC rods, the GVD as well as the TOD values can be arranged appropriately. For this reason, we increase the number of auxiliary rods from single to double, in the proposed structure thus the PC transforms into C_2 symmetry structure.

The introduced double auxiliary rods are placed in 0° and 180° with respect to the main PC rod in counterclockwise (CCW) direction in the unit cell, as seen in Fig. 1(g). The distance between main rod and auxiliary rods are taken the same value of C_1 symmetry structure ($d=0.38a$). The radii of auxiliary rods are fixed to $r=0.12a$. The EFCs of 3rd, 4th and 5th TM polarization bands are also calculated and presented in Figs. 4(a), 4(b) and 4(c), respectively. The schematics of corresponding PC unit cell are given as insets in the corresponding figure plots. The frequency contours calculated for 3rd TM band exhibits curved nonlinear shapes. On the other hand, the linear contours are provided by the EFC of the 4th and 5th bands, as shown in Figs. 4(b) and 4(c), respectively. As expected, change in the overall index contrast of the hexagonal lattice PC unit cell by introducing double auxiliary rods played an important role in revealing all-angle SC effect. These auxiliary rods located at 0° and 180° angles with respect to the main PC rod, serve as a physical connection between the main rods in the PC structure which enables the incident light to propagate straightly. The perfect linear contour for the incident light at all angles is observed at the frequency range between $a/\lambda=0.616$ and $a/\lambda=0.656$ in Fig. 4(b). This indicates that the PC structure with C_2 group symmetry provides all-angle SC effect at the frequency interval with the broad bandwidth of $\Delta\omega/\omega_c=6.3\%$, which is 2.63 times greater than bandwidth of SC in C_1 group symmetry structure. Moreover, EFC of 5th TM band given in Fig. 4(c) presents all-angle SC effect for the frequency range between $a/\lambda=0.712$ and $a/\lambda=0.760$ with a bandwidth of $\Delta\omega/\omega_c=6.5\%$. Therefore, we can say that C_2 symmetry structure operates as all-angle self-collimator at two different frequency bands with the wider frequency bandwidths compared to C_∞ and C_1 symmetry structures.

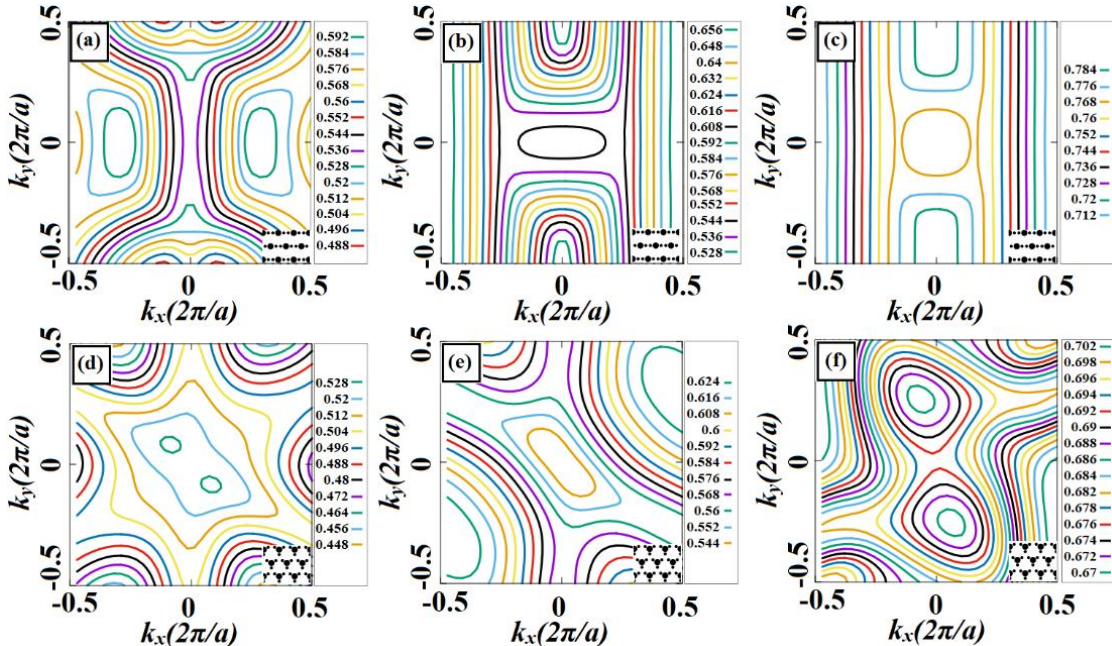


Figure 4. EFC plots of the hexagonal PC structure with two dielectric rods (C_2 symmetric structure) for (a) the 3rd, (b) the 4th and (c) the 5th TM bands. EFCs for the hexagonal PC structure with three auxiliary dielectric rods (C_3 symmetric structure) for (a) the 3rd, (b) the 4th and (c) the 5th TM bands.

To increase index contrast even more, the number of auxiliary rods is increased into three and placed at the angles of 30° , 150° and 270° with respect to the main PC rod in a CCW direction constituting C_3 symmetry group structure as shown in Fig. 1(h). Here opto-geometrical parameters used for the C_∞ , C_1 and C_2 structures are also valid for C_3 group. The EFCs calculated for 3rd, 4th and 5th TM polarization bands of C_3 symmetry group structure are given in Figs. 4(d), 4(e) and 4(f), respectively. However, this structure doesn't yield any sign of self-collimation effect as can be inferred from the EFCs because C_3 group symmetry is more complex and sensitive for scattering and diffraction compared to the C_2 and C_∞ , C_1 symmetry groups. As a result, C_3 group exhibits a complex/nonlinear shaped frequency response that reflected in EFCs.

To qualitatively evaluate all-angle SC characteristics of the designed C_2 symmetry group, corresponding steady-state intensity distributions are calculated and presented in Figs. 5(a)-5(c) and Figs. 5(d)-5(f) for 4th and 5th TM polarization bands, respectively. The results of the steady-state intensity field profiles calculated for the operating frequencies of $a/\lambda = 0.62$, $a/\lambda = 0.63$, and $a/\lambda = 0.64$ are given in Figs. 5(a), 5(b) and 5(c), respectively. It is important to note that these frequencies are lying within the all-angle SC frequency range of $a/\lambda = 0.616$ - 0.656 (see Fig. 4(b), EFCs for 4th TM band). From the intensity distributions one can observe light propagation with negligible broadening while keeping strong confinement of the energy at the center of the structure. Even though the light propagates without spatial expansion, the light is not propagating inside the PC structure by keeping intact the spatial width of the source. In other words, light propagates inside the structure by concentrating large amount of energy at the center of the PC accompanied with the trace of the residual energy wave. On the other hand, in the case of 5th band, the steady-state intensity profiles of propagating wave operating at frequencies of $a/\lambda = 0.73$, $a/\lambda = 0.74$, and $a/\lambda = 0.75$ exhibit less scattered distribution of the collimated beam as shown in Figs. 5(d), 5(e) and 5(f), respectively.

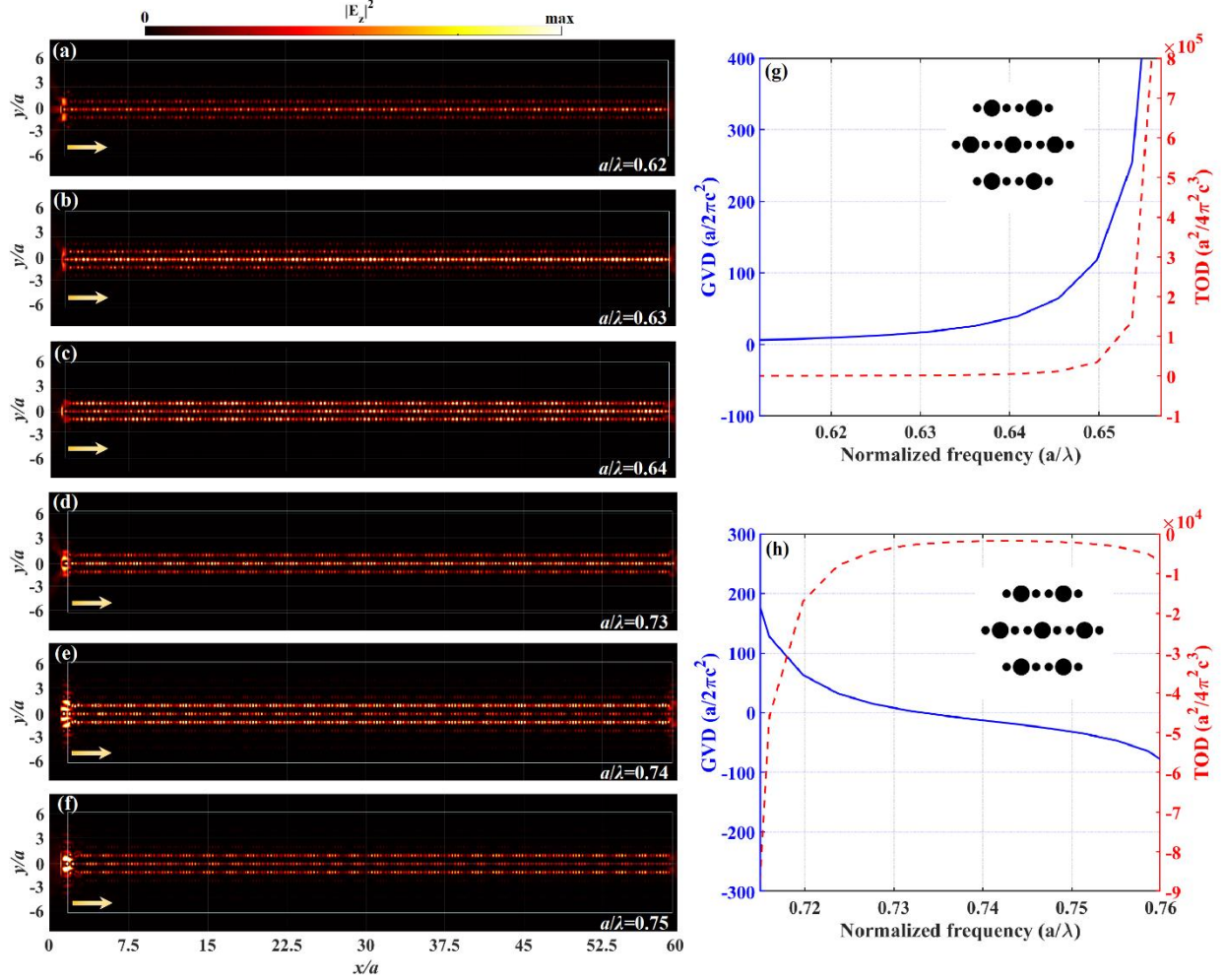


Figure 5. Steady-state electric field intensity distributions of C_2 group symmetry PC structure operating at the frequencies of (a) $a/\lambda=0.620$, (b) $a/\lambda=0.630$ and (c) $a/\lambda=0.640$ in the 4th TM band. Steady-state electric field intensity distributions of the same structure operating at 5th TM band of (d) $a/\lambda=0.730$, (e) $a/\lambda=0.740$ and (f) $a/\lambda=0.750$. Variation of the GVD and TOD values for the C_2 symmetry group PC structure as a function of normalized frequency at (g) the 4th and (h) the 5th TM bands, with representation of unit cell schematic as an inset.

Similarly, the values of GVD and TOD are also calculated for the 4th and 5th bands as given in Figs. 5(g) and 5(h), respectively. In these graphs, it can be observed that the GVD and TOD values vary between $7.3 (a/2\pi c^2) - 254.3 (a/2\pi c^2)$ and $449.2 (a^2/4\pi^2 c^3) - 1.3 \times 10^5 (a^2/4\pi^2 c^3)$ for the TM 4th band, respectively, and between $182.5 (a/2\pi c^2) - 71.3 (a/2\pi c^2)$ and $-24380(a^2/4\pi^2 c^3) - 9619 (a^2/4\pi^2 c^3)$ for the TM 5th band values. Here GVD and TOD values are smaller comparing to those values in C_1 symmetry group case. On the other hand, the variation of GVD values in 4th band is much more noticeable comparing to variation of GVD in 5th band. It shows that C_2 symmetry group PC structure is more sensitive for the frequency change at the 4th band which can be observed from steady-state electric field intensity profiles given in Figs. 5(a)-5(c).

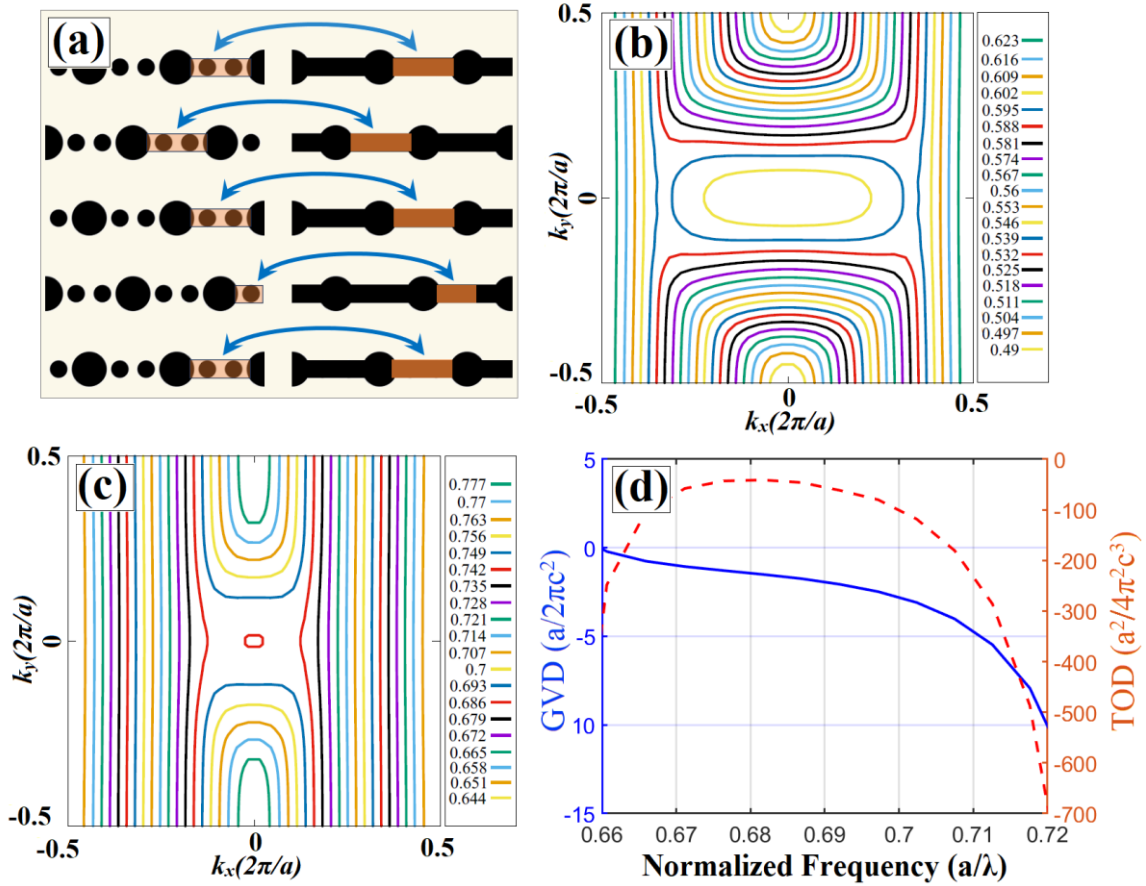


Figure 6. (a) Schematic view of the proposed the hybrid PC structure transformed/adapted from C_2 group symmetry structure. EFC diagrams of the hybrid structure for (b) the 4th and (c) the 5th TM bands. (d) Variations of the GVD and TOD values for the hybrid PC structure as a function of normalized frequencies at the 5th TM bands.

It is important to note that the designed PC structure should present efficient optical performance as well as high compatibility with the state-of-the-art fabrication techniques. Here, C_2 symmetry group structure presents the desired all-angle SC characteristics working in a broadband frequency range. However, the C_2 group symmetry structure with the isolated auxiliary rods and the main rods can be challenging for the high precision fabrications [41]. On the other hand, if we look to the C_2 group symmetry one can observe that auxiliary rods around the main rod ($\theta=0^\circ$) can be placed in a very close distance (auxiliary rods can touch the main rod) to the main rod. This situation can be beneficial in terms of generating composite/hybrid structure that can exhibit similar optical characteristics. The composite PC structure that generated using C_2 group symmetry ($\theta=0^\circ$) is shown in Fig. 6(a), two auxiliary rods are replaced by rectangular photonic wire having width equal to the diameter of auxiliary rods and the same refractive index. Here, photonic wire acts as connecting bridge between isolated main rods and is not violating the C_2 group symmetry. As a result, hybrid structure resembles C_2 group symmetry and is considerably more robust against possible fabrication precision issues. As depicted in Figs. 6(b) and 6(c), this hybrid structure exhibits all-angle self-collimation characteristics at the 4th and 5th TM bands like C_2 group symmetry PC structure. The hybrid PC structure exhibits near-zero GVD and TOD performance

as shown in Fig. 6(d), which can be used to tune the electromagnetic pulse structure to maintain signal fidelity. Furthermore, these near-zero values can be used for further data compression or energy transfer of the wave packet. In addition, the combination of negative TOD with near-zero values can be utilized to shape the wave packet. The hybrid structure also inherits the significant SC potential of the two auxiliary rod structures, as seen in both the EFC contours in Fig. 6 (b) and 6(c) and the steady-state electric field intensity distribution in Fig. 7.

In Fig. 7 corresponding steady-state electric field intensity distributions for the 4th and 5th TM polarization bands are calculated to qualitatively evaluate the all-angle self-collimation properties of the designed hybrid symmetry structure. The steady-state intensity field profiles for the selected frequencies operating at $a/\lambda=0.665$, $a/\lambda=0.675$, $a/\lambda=0.685$, $a/\lambda=0.695$, $a/\lambda=0.705$ and $a/\lambda=0.715$ are demonstrated in Figs. 7(a), 7(b), 7(c), 7(d), 7(e) and 7(f), respectively. It is important to note that these frequencies are within the all-angle SC frequencies of $a/\lambda=0.648$ - 0.736 as noticed in Fig. 6(c). As a result, proposed hybrid PC structure demonstrates all-angle SC effect with negligible broadening and spatial deterioration while ensuring strong confinement of energy at the center of the structure.

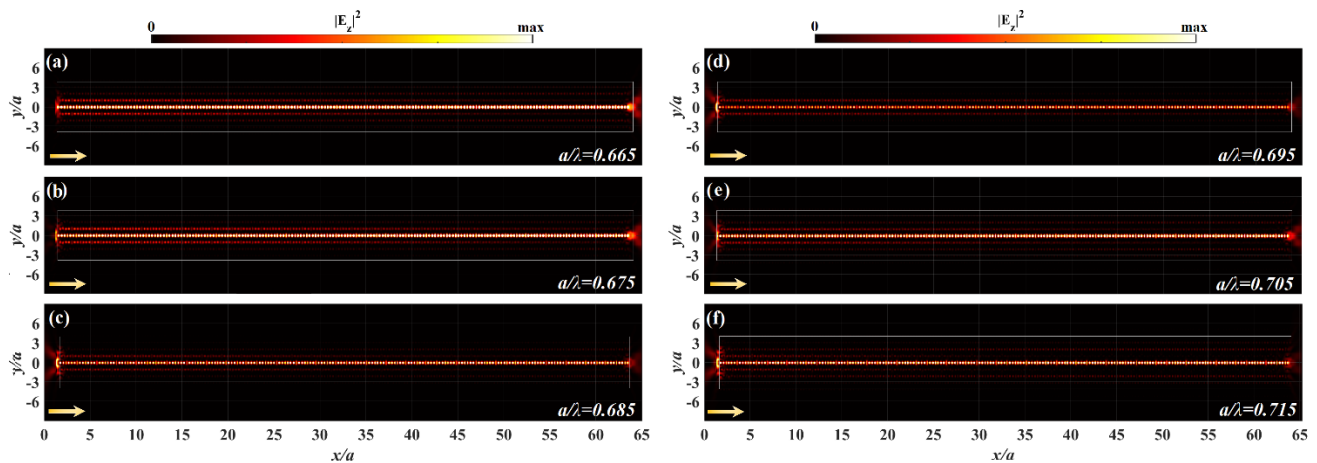


Figure 7. Steady-state electric field intensity distributions of hybrid PC structure operating at the frequencies of (a) $a/\lambda=0.665$, (b) $a/\lambda=0.675$, (c) $a/\lambda=0.685$, (d) $a/\lambda=0.695$, (e) $a/\lambda=0.705$ and (f) $a/\lambda=0.715$ in the 5th TM band.

4. Conclusion

In this study, we introduce a PC structure with a hexagonal lattice, where adjustments in unit cell symmetry reveal a comprehensive all-angle SC effect. By optimizing opto-geometric parameters, such as the rotational angle of auxiliary rods and adjacent distances, we conduct a thorough analysis of the SC property, utilizing group velocity dispersion (GVD) and third-order dispersion (TOD) characteristics. Furthermore, we explore the interplay between symmetry properties and their impact on dispersion characteristics. Symmetry manipulation affords us a profound understanding of the underlying mechanisms governing light collimation and confinement in these

configurations. The PC structure with a C_1 symmetry group exhibits an all-angle SC effect within a normalized frequency range of $a/\lambda=0.652$ to $a/\lambda=0.668$, featuring a bandwidth of $\Delta\omega/\omega = 2.4\%$. Breaking symmetry further by transitioning from C_1 to C_2 group symmetry enhances the SC bandwidth to $\Delta\omega/\omega=6.5\%$. It unveils perfect linear EFCs at two frequency bands: all-angle SC between $a/\lambda=0.616$ and $a/\lambda=0.656$ in the 4th TM band and between $a/\lambda=0.712$ and $a/\lambda=0.760$ in the 5th TM band. In this context, we present and analyze GVD and TOD values variations within specific ranges for both the TM 4th and 5th bands to enhance our understanding of these dispersion characteristics. Additionally, we propose a hybrid PC structure resembling C_2 group symmetry, where rectangular photonic wires, matching the diameter of auxiliary rods and sharing the same refractive index, replace two auxiliary rods. This hybrid structure features an all-angle SC effect with an operating bandwidth of $\Delta\omega/\omega=11.7\%$, coupled with near-zero GVD and TOD performance. To the best of our knowledge, this study provides the first comprehensive analysis of all-angle SC characteristics in low-symmetry PC structures arranged in hexagonal lattices using the EFC engineering approach.

Acknowledgment

This work was supported by Pamukkale University - Scientific Research Project Unit under Project No: BAP-2021FEBE040 and the Scientific and Technological Research Council of Turkey (TUBITAK) under Project No. 1218E954. Z.M.Y. acknowledges YÖK (Council of Higher Education) 100/2000 Project Program for the financial support. Authors would like to thank Assoc. Prof. Dr. Sami Sözüer for valuable discussions on generating of EFC for hexagonal PC structures and for Berkay Neşeli for his proof reading of the manuscript.

References

- [1] Yablonovitch, E. (1987). "Inhibited Spontaneous Emission in Solid-State Physics and Electronics." *Physical Review Letters*, 58(20), 2059–2062. doi:10.1103/physrevlett.58.2059
- [2] John, S. (1987). "Strong localization of photons in certain disordered dielectric superlattices." *Physical Review Letters*, 58(23), 2486–2489. doi:10.1103/physrevlett.58.2486
- [3] Koshiba, M. (2001). "Wavelength division multiplexing and demultiplexing with photonic crystal waveguide couplers." *Journal of Lightwave Technology*, 19(12), 1970–1975. doi:10.1109/50.971693
- [4] Tekeste, M. Y., Yarrison-Rice, J. M. (2006). "High efficiency photonic crystal-based wavelength demultiplexer." *Optics Express*, 14(17), 7931. doi:10.1364/oe.14.007931
- [5] Cubukcu, E., Aydin, K., Ozbay, E., Foteinopoulou, S. & Soukoulis, C. M. Electromagnetic waves: Negative refraction by photonic crystals. *Nature* 423, 604 (2003).
- [6] M. Gumus, I. H. Giden, O. Akcaalan, M. Turduev, and H. Kurt, "Enhanced superprism effect in symmetry reduced photonic crystals", *Appl. Phys. Lett.* 113, 131103 (2018) <https://doi.org/10.1063/1.5032197>

- [7] Wu, Z. H., Xie, K., Yang, H. J., Jiang, P., He, X. J. (2011). "All-angle self-collimation in two-dimensional rhombic-lattice photonic crystals." *Journal of Optics*, 14(1), 015002. doi:10.1088/2040-8978/14/1/015002
- [8] T. Sato *et al.*, "Photonic Crystal Lasers for Chip-to-Chip and On-Chip Optical Interconnects," in *IEEE Journal of Selected Topics in Quantum Electronics*, vol. 21, no. 6, pp. 728-737, Nov.-Dec. 2015, Art no. 4900410, doi: 10.1109/JSTQE.2015.2420991.
- [9] Chuang, Y.-C., Suleski, T. J. (2011). "Photonic crystals for broadband, omnidirectional self-collimation." *Journal of Optics*, 13(3), 035103. doi:10.1088/2040-8978/13/3/035103
- [10] Yasa, Utku Gorkem et al. "High Extinction Ratio Polarization Beam Splitter Design by Low-Symmetric Photonic Crystals." *Journal of Lightwave Technology* 35 (2017): 1677-1683.
- [11] Noori M., Soroosh M., Baghban H., (2015). "All-angle self-collimation in two-dimensional square array photonic crystals based on index contrast tailoring," *Opt. Eng.* 54(3) 037111 <https://doi.org/10.1117/1.OE.54.3.037111> .
- [12] Noori, M., Soroosh, M. (2015). "A comprehensive comparison of photonic band gap and self-collimation based 2D square array waveguides." *Optik-International Journal for Light and Electron Optics*, 126(23), 4775–4781. doi: 10.1016/j.ijleo.2015.08.082
- [13] Prather, D. W., Shi, S., Murakowski, J., Schneider, G. J., Sharkawy, A., Chen, C., Martin, R. (2007). "Self-collimation in photonic crystal structures: a new paradigm for applications and device development." *Journal of Physics D: Applied Physics*, 40(9), 2635–2651. doi:10.1088/0022-3727/40/9/s04
- [14] Yifeng, S., Lulu, L., Hao, Z., Yueqin, C. (2014). "Enhanced beaming of light from a photonic crystal waveguide via a self-collimation photonic crystal." *Optik-International Journal for Light and Electron Optics*, 125(10), 2217–2219. doi: 10.1016/j.ijleo.2013.10.053
- [15] Feng, S., Lv, M., Qu, Z., Chen, X., Wang, Y., Wang, W. (2012). "Polarization Beam Splitter Based on the Self-Collimation of the Two-Dimensional Metallic Photonic Crystal." 2012 Symposium on Photonics and Optoelectronics. doi:10.1109/sopo.2012.6270935
- [16] Ren, K., Ren, X. (2012). "Y-shaped beam splitter by graded structure design in a photonic crystal." *Chinese Science Bulletin*, 57(11), 1241–1245. doi:10.1007/s11434-012-5007-4
- [17] Noori, M., Soroosh, M., Baghban, H. (2016). "Design of highly efficient polarization beam splitter based on self-collimation on Si platform." *Journal of Modern Optics*, 64(5), 491–499. doi:10.1080/09500340.2016.1244294
- [18] Christina, X. S., Kabilan, A. P. (2012). "Design of optical logic gates using self-collimated beams in 2D photonic crystal." *Photonic Sensors*, 2(2), 173–179. doi:10.1007/s13320-012-0054-

- [19] Zhang, Y., Zhang, Y., Li, B. (2007). "Optical switches and logic gates based on self-collimated beams in two-dimensional photonic crystals." *Optics Express*, 15(15), 9287. doi:10.1364/oe.15.009287
- [20] Wang, Y., Wang, H., Xue, Q., Zheng, W. (2012). "Photonic crystal self-collimation sensor." *Optics Express*, 20(11), 12111. doi:10.1364/oe.20.012111
- [21] Turduev, M., Giden, I. H., Kurt, H. (2013). "Extraordinary wavelength dependence of self-collimation effect in photonic crystal with low structural symmetry." *Photonics and Nanostructures - Fundamentals and Applications*, 11(3), 241–252. doi: 10.1016/j.photonics.2013.04.004
- [22] Zheng, G., Wang, Z., Zhao, D., Zhang, W., Liu, Y. (2014). "Wavelength-division-multiplexing system with photonic crystal self-collimation and co-directional coupling effect." *Optik- International Journal for Light and Electron Optics*, 125(11), 2638–2641. doi: 10.1016/j.ijleo.2013.11.034
- [23] Giden, I. H., Turduev, M., Kurt, H. (2014). 'Reduced Symmetry and Analogy to Chirality in Periodic Dielectric Media'. *Journal of the European Optical Society. Rapid Publications*, vol. 9, no. 14045i, European Optical Society, <https://doi.org/10.2971/jeos.2014.14045i>.
- [24] Jovanović, D., Gajic R. (2011). Optical properties of the (3.4.6.4) hexagonal Archimedean photonic crystal. *Journal of Nanophotonics*, 5(1), 051820. doi:10.1117/1.3611019
- [25] Grimmer, Hans. (2017). *Symmetry and Physical Properties of Crystals*. By Cécile Malgrange, Christian Ricolleau and Michel Schlenker. *Acta Crystallographica Section A*. 73. 279-280.
- [26] Giden, I. H., Turduev, M., Kurt, H., 2013. "Broadband super-collimation with low-symmetric photonic crystal". *Photonics and Nanostructures - Fundamentals and Applications*, 11, 132–138.
- [27] Melike A Gumus, Mediha Tutgun, Döne Yılmaz, and Hamza Kurt. ,2019, A reduced symmetric 2d photonic crystal cavity with wavelength tunability. *Journal of Physics D: Applied Physics*, 52(32):325103.
- [28] Johnson, S., Joannopoulos, J. (2001). "Block-iterative frequency-domain methods for Maxwell's equations in a planewave basis." *Optics Express*, 8(3), 173. doi:10.1364/oe.8.000173
- [29] S.Guo, S.Albin, "Simple plane wave implementation for photonic crystal calculations", *Optics Express* 11, no.2, p.167-175, 2003.
- [30] J.D. Joannopoulos, R.D. Meade, and J.N. Winn, "Photonic crystals, Molding the flow of light", Princeton University Press, 1995.
- [31] Rumpf, R. C. (2006). "Design and optimization of nano-optical elements by coupling fabrication to optical behavior." Ph.D. Dissertation, The University of Central Florida
- [32] Deng, J., Guasch, O., & Zheng, L. (2021). Reconstructed Gaussian basis to characterize flexural wave collimation in plates with periodic arrays of annular acoustic black

holes. *International Journal of Mechanical Sciences*, 194(106179), 106179. doi: 10.1016/j.ijmecsci.2020.106179

[33] Hideo Kosaka, Takayuki Kawashima, Akihisa Tomita, Masaya Notomi, Toshiaki Tamamura, Takashi Sato, and Shojiro Kawakami. Self-collimating phenomena in photonic crystals. *Applied Physics Letters*, 74:1212–1214, 1999.

[34] A. Taflove and S. C. Hagness, *Computational Electrodynamics: The Finite-Difference Time-Domain Method*, 3rd ed. (Artech House, Boston, 2005).

[35] Lumerical FDTD Solutions, Inc. <http://www.lumerical.com>.

[36] Berenger, J. P. (1994). "A perfectly matched layer for the absorption of electromagnetic waves." *Journal of Computational Physics*, 114(2), 185–200. doi:10.1006/jcph.1994.1159

[37] Jelena Vucković, Marko Loncar, Hideo Mabuchi, and Axel Scherer. Design of photonic crystal microcavities for cavity qed. *Phys. Rev. E*, 65:016608, Dec 2001.

[38] Hamam, R. E., Ibanescu, M., Johnson, S. G., Joannopoulos, J. D., and Soljačić, M., "Broadband super-collimation in a hybrid photonic crystal structure," *Opt. Express* 17, 8109-8118 (2009)

[39] Chuanhong Zhou, Qian Gong, Peijun Yao, Deyin Zhao, Xunya Jiang; Bulletlike light pulses in photonic crystals. *Appl. Phys. Lett.* 11 August 2008; 93 (6): 061103.

[40] Chuan C. Cheng, Axel Scherer, Rong-Chung Tyan, Yeshayahu Fainman, George Witzgall, Eli Yablonovitch; New fabrication techniques for high quality photonic crystals. *Journal of Vacuum Science & Technology B: Microelectronics and Nanometer Structures Processing, Measurement, and Phenomena* 1 November 1997; 15 (6): 2764–2767.